ISBN: 978-3-95450-132-8 doi:10.18429/JACoW-IPAC2014-WEPME004

PREDICTION OF SEVERE ELECTRON LOADING OF HIGH-GRADIENT ACCELERATING STRUCTURES BASED ON FIELD EMISSION MEASUREMENTS OF NB AND CU SAMPLES

S. Lagotzky*, G. Müller, FB C Physics Department, University of Wuppertal, 42097, Germany

Abstract

A statistical model for the activation-field dependence of the observed electron field emission from metallic samples is presented here. The activation of particulates and surface defects is explained by the transition from a MIM and MIV to a geometric field enhancement emission process. Based on an exponential field enhancement factor distribution, an exponential-like dependence of the emitter number density *N* on the activation field was derived. There are only two input parameters in the model, which depend on the surface quality. Systematic FESM measurements on numerous Nb and Cu samples have confirmed the expected field-scaling of *N* of the statistical model. Therefore, a prediction of the electron loading of actual (XFEL) and future (ILC, CLIC) accelerating structures at their design field gradients is possible using an estimated high-field area. The achieved surface quality of superconducting Nb might be sufficient for XFEL but not for ILC. Much more effort, however, will be required to reduce the electron loading and breakdown events in the Cu structures for CLIC.

INTRODUCTION

Enhanced field emission (EFE) of electrons often limits the achievable gradients of superconducting (XFEL, ILC) and normal conducting (CLIC) accelerating structures. Experiences with the cavity mass production for the XFEL at DESY (Hamburg) have shown that at least 30% of the fabricated nine-cell Nb cavities need to be retreated mainly because of EFE [1] to achieve the required specifications. In case of the actual multi-cell Cu structures for CLIC, EFE is considered as major origin of the electron loading and breakdown events, which often lead to severe damage of the cavity surface. Field emission scanning microscopy (FESM) and correlated SEM/EDX measurements of relevant Nb and Cu samples revealed particulates and surface defects with field enhancement factors β = 10 - 120 as main origin of EFE [2]-[4]. The number density of emitters *N* strongly increased with the applied electric activation field E_{act}, and FESM results on polycrystalline Nb suggested an exponential increase of $N(E_{act})$ [5]. Such a scaling law would be most important to estimate the EFE of high-gradient accelerating structures at surface fields, which are usually much lower than the typical test fields of similarly prepared samples. Therefore, we have set up here a statistical model for the activation of EFE on metallic surfaces. The resulting $N(E_{act})$ scaling law will be verified by the recent EFE measurements on Nb and Cu samples.

*s.lagotzky@uni-wuppertal.de

STATISTICAL MODEL

For most emitters on Nb and Cu samples, EFE activation is observed at E_{act} resulting in a significantly reduced onset field E_{on}(1nA). This phenomenon can be explained by the presence of an insulating oxide layer (IOL) of thickness d_{ox} (~ few nm) on top of the metallic bulk [3]. Accordingly, surface defects initially form a metal-insulator-vacuum (MIV) and particulates a metal-insulator-metal (MIM) emission regime [6], for which the field enhancement is given by $\beta_{MIV}^{act} \approx h_s/r_s$ and $\beta_{MIM}^{act} \approx h_p/d_{ox}$ (see Fig. 1). As result of the activated emission current, a conducting channel (CC) is usually burned into the oxide, which then provides EFE due to geometric field enhancement, i.e. at a modified $\beta_s^{on} \approx (h_s/r_s) \cdot (h_c/r_c)$ and $\beta_p^{on} \approx (h_p/r_p)$ for surface defects and particulates, respectively (see Fig. 1). It is remarkable that surface defects always get stronger ($\beta_s^{on} > \beta_{MIV}^{act}$) by activation, while only those particulates with $r_p < d_{ox}$ might continue with EFE.

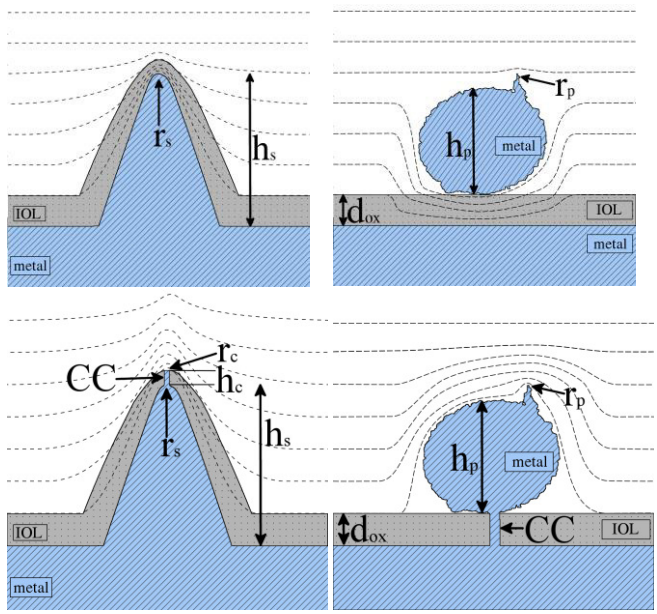

Figure 1: Equipotential lines for a surface protrusion of height h_s with apex radius r_s (left) and a rough particulate of height h_p with apex radius r_p (right) before (top) and after (bottom) creation of a conducting channel (CC) of height h_c with apex radius r_c into the insulating oxide layer (IOL).

ISBN: 978-3-95450-132-8 doi:10.18429/JACoW-IPAC2014-WEPME004

For both types of emitters, EFE will finally occur if the locally enhanced field is above a specific field limit E_{lim}

$$\beta^{act} \cdot E_{act} \geq E_{lim} \quad (1)$$

which depends on the dielectric breakdown of the IOL in dc measurements and probably on the microwave losses in rf cavities, too. In order to calculate N at a given E_{act}, all activated emitters that fulfil (1) must be included:

$$N(E_{act}) = \int_{E_{lim}/E_{act}}^{\infty} N(\beta^{act}) d\beta^{act} \quad (2)$$

The distribution function $N(\beta^{act})$ of real surface defects and particulates is not known yet, but as reasonable approach for a first statistical EFE model by H. Padamsee et al. [7] an exponential dependence was assumed

$$N(\beta^{act}) = N_0 \cdot \exp\left(-c_s \cdot \beta^{act}\right) \quad (3)$$

where N_0 is a normalization factor and c_s depends on the actual surface condition, i.e. the shape of particulates and surface defects. Combination of (2) and (3) leads to

$$N(E_{act}) = N_{tot} \cdot \exp(c_s) \cdot \exp\left(-c_s \frac{E_{lim}}{E_{act}}\right) \quad (4)$$

where N_{tot} is linked to N_0 and c_s by

$$N_{tot} = N_0 \cdot \int_1^{\infty} \exp(-c_s \cdot \beta) d\beta = \frac{N_0}{c_s} \cdot \exp(-c_s) \quad (5)$$

The resulting shape of (3) and (4) for different N_{tot} and c_s values is shown in Fig. 2. At low fields the $N(E_{act})$ curves always start from 0 due to the inverse field dependence, followed by an exponential-like increase and a saturation towards N_{tot} which is only reached for $E_{act} = E_{lim}$. Overall, measured data should be fitted by using

$$\ln(N) = A + B \cdot E^{-1} \quad (6)$$

with $A = \ln(N_{tot}) + c_s$ and $B = c_s \cdot E_{lim}$.

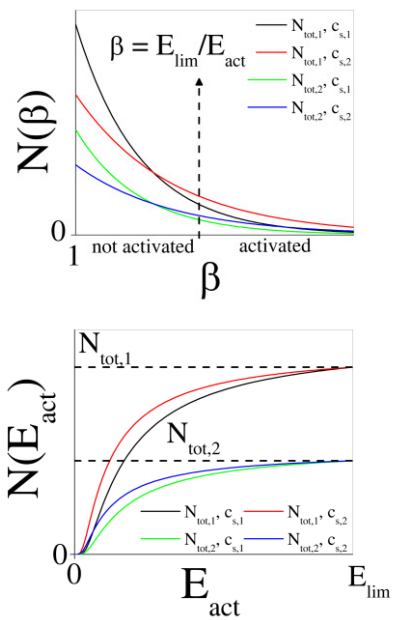

Figure 2: Influence of the distribution function $N(\beta)$ (top) on the $N(E_{act})$ scaling (bottom) for $N_{tot,1} > N_{tot,2}$ and $c_{s,1} > c_{s,2}$.

VERIFICATION BY MEASUREMENTS

Single Crystal Nb

The EFE activation of four dry-ice-cleaned (DIC) single crystal (SC) Nb samples which got first buffered chemical polishing (BCP, 20-120 µm) and then electropolishing (EP, 116-18 µm) with different EP/BCP ratios ρ_p (0.15, 0.73, 2.40, 5.80) was systematically measured with the FESM [8]. Since there was no dependence of $N(E_{act})$ on ρ_p, the results were summarized to reduce the statistical error as shown in Fig. 3. Obviously, the statistical model equation (6) describes the data quite well (correlation coefficient R = -0.99333). By means of the least square fit parameters A and B, down-scaling to much lower E_{peak} is possible resulting in $N = (1.48 \pm 0.76) \times 10^{-2}$/cm^2 for ILC and $N = (1.60 \pm 1.18) \times 10^{-4}$ cm^{-2} for XFEL design fields. Assuming a high-field (> $0.9 \times E_{peak}$) iris area of 22 cm^2 for each cell of a superconducting 1.3 GHz nine-cell structure, even 3 % of SC XFEL structures would suffer from EFE after DIC, and much more effort would be required for the realization of the envisaged ILC field gradient [9].

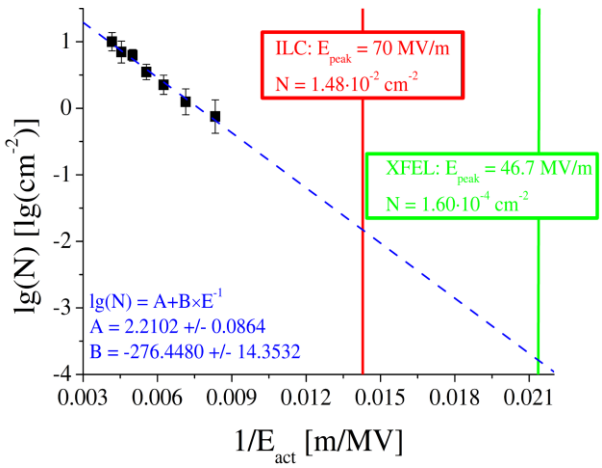

Figure 3: Measured $N(E_{act})$ for DIC SC Nb with line fit according to (6) and extrapolation to E_{peak} of XFEL/ILC.

Heat Treated Large Grain & SC Nb

In-situ heat treatments (HT) of large grain (LG) and SC Nb after BCP (40 µm), EP (140 µm) and high-pressure rinsing (HPR) leads to activation of EFE due to dissolution of the IOL (Nb_2O_5) [3]. Recent EFE results of four LG and SC samples (40 µm BCP, 140 µm EP) after HT between 122°C and 400°C for 2 – 24 h [10] are shown in Fig. 4. Fits of the measured data to the statistical model equation (6) are adequate within the error bars (R = -0.82119, -0.82199, -0.98314, and -0.99962 for initial, 122°C, 200°C, and 400° HT, resp.). Down-scaling of $N(E_{act})$ to ILC requirements (E_{act} = 70 MV/m) results in $N = (1.64 \pm 2.19) \times 10^{-1}$ cm^{-2} after the HT at 122°C for 24 h, which is part of the actual cavity fabrication process. Therefore, thicker IOL might be helpful to avoid EFE sufficiently for ILC.

ISBN: 978-3-95450-132-8 doi:10.18429/JACoW-IPAC2014-WEPME004

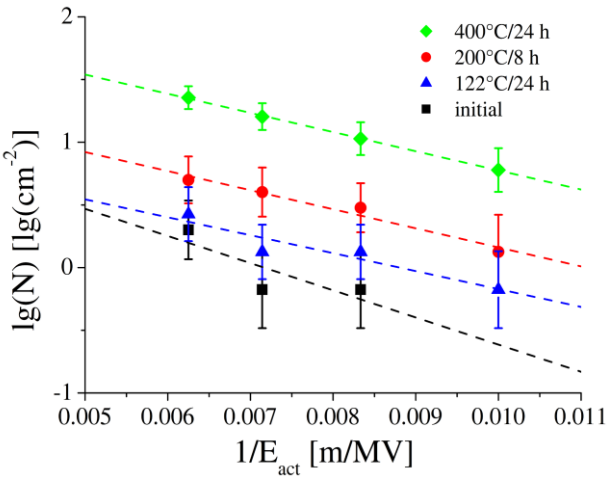

Figure 4: Measured $N(E_{act})$ for HPR LG/SC Nb after various HT with lines fits according to (6).

Polycrystalline Cu

FESM measurements of five diamond-turned (DT) and partially etched Cu sampless before and after DIC revealed a similar EFE activation as for Nb [4]. Figure 5 shows the results of the measurements as well as the fits. Here again the fit quality to the statistical model equation (6) is rather good (R = -0.89839 for DT, R = -0.9514 for DT & DIC, and R = -0.97768 for DT & etched & DIC). Accordingly, DIC reduces N at the peak surface field relevant for CLIC (E_{peak} = 243 MV/m) by a factor of about 4.2 from N = 125/cm^2 to N = 29/cm^2 while additionally etching does not show any noticeable effect on the EFE activation. Therefore, the surface preparation of normal conducting 11.2 GHz CLIC structures must be significantly improved for the suppression of EFE and breakdown events.

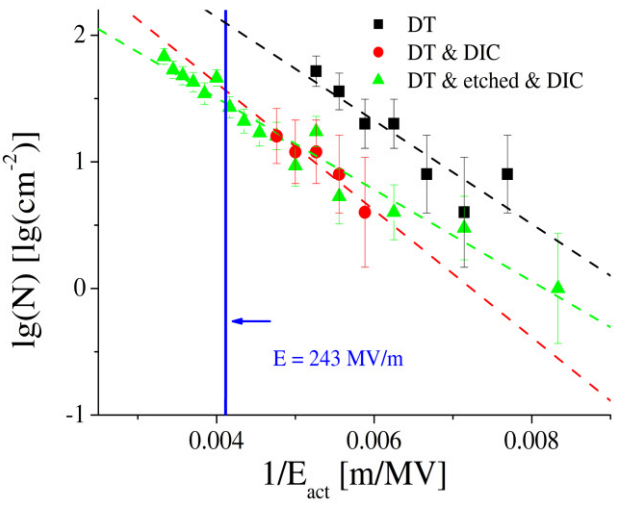

Figure 5: Measured $N(E_{act})$ dependence for differently prepared polycrystalline Cu with line fits according to (6).

CONCLUSION

The statistical model presented here is well suited to describe the activation-field dependence of the measured emitter number density on flat metallic surfaces. Therefore, it can be used to predict the electron loading of high-gradient accelerating structures at their design field levels. Nevertheless, a reduction of the statistical error of sample measurements would be helpful to improve the scaling. Based on this model and recent FESM results it becomes obvious why a significant part of the actual 1.3 GHz nine-cell Nb structures for XFEL suffer from EFE, and that even the use of SC and DIC would not remove EFE completely.

Therefore, alternative solutions must be found for the EFE reduction in the superconducting accelerating cavities for ILC, e.g. improved preparation and cleaning techniques, careful handling to avoid any surface damage, or advanced emitter processing. In comparison, the FESM results of the normal conducting Cu samples show that severe EFE will occur in the 11.2 GHz Cu accelerating structures of CLIC. Therefore, the surface quality must be further improved to reduce the electron loading and breakdown events.

The statistical model is yet based on an exponential field enhancement distribution $N(\beta)$ with two parameters which should be verified or modified for surface defects and particulates by means of surface analysis techniques. The influence of the IOL thickness on N_{tot} and c_s has also to be taken into account then. Moreover, the EFE scaling for actual accelerating structures could be improved by use of a weighted averaging based on their real field distribution.

ACKNOWLEDGMENT

This work is funded by the German BMBF under project number 05H12PX6.

REFERENCES

[1] D. Reschke, THIOA01, Proc. SRF2013.
[2] A. Dangwal et al., Phys. Rev. ST Accel. Beams 12, 023501 (2009).
[3] A. Navitski et al., Phys. Rev. ST Accel. Beams 16, 112001 (2013).
[4] S. Lagotzky et al., WEPME005, IPAC2014.
[5] A. Navitski, PhD thesis, Univ. of Wuppertal (2010).
[6] R. V. Latham, *High Voltage Vacuum Insulation*, Academic Press, London (1995).
[7] Padamsee et al., p. 998, Proc. PAC1993.
[8] S. Lagotzky et al., TUP093, Proc. SRF2013.
[9] ILC Technical Design Report (2013).
[10] S. Lagotzky et al., TUP094, Proc. SRF2013.